

A novel method for net-shape manufacturing of metal–metal sulfide cermets

Atefeh Nabavi · Alexander Capozzi ·
Samuel Goroshin · David L. Frost ·
Francois Barthelat

Received: 16 April 2014 / Accepted: 28 July 2014 / Published online: 9 August 2014
© Springer Science+Business Media New York 2014

Abstract Ceramic–metal composites (cermets) offer unique combinations of hardness and toughness, which make them attractive for a variety of applications. In this study, we propose a new method for the preparation of the metal–sulfur precursor mixture based on the ability to melt-cast the precursor mixture. We have used self-propagating high-temperature synthesis to produce a chromium/chromium sulfide cermet, exploiting the fact that this mixture of metal and sulfur can support the propagation of reactive waves. This ability, together with the properties of the reaction products (low gas evolution and liquid sulfide products), enables the net-shape synthesis of dense, near theoretical density product with a relatively simple and low-cost set-up. While the thermochemical calculations predict near-zero gas production for the chromium–sulfur system, the actual cermets showed a large amount of porosity (about 70 %), when synthesized at atmospheric pressure. The possible sources for porosity were identified, and the process improved to bring the porosity down to about 7 %. We also investigated the physical properties of the produced cermet with optical microscopy, scanning electron microscopy, energy dispersive X-ray spectroscopy, and X-ray diffraction techniques.

Introduction

Metal sulfide composites are in high demand in the chemical, metallurgical, and electrical industries because

of attractive characteristics such as hardness, magnetic properties, semi-conductivity, electroluminescence, infrared transparency, and catalytic properties [1–4]. Current manufacturing methods for metal sulfides usually involve one of two different principal methods, including a complex multistage wet chemical process involving the precipitation of the corresponding salts from an aqueous solution with hydrogen sulfide, or hot sintering of the respective elemental reactant powders in a resistive furnace in a high-pressure inert or hydrogen sulfide atmosphere [2]. These conventional methods for synthesizing ceramic–metal composites are complex, time and energy consuming, and environmentally harmful. In addition, these methods do not allow the fabrication of articles with complex shapes. Self-propagating high-temperature synthesis (SHS) offers an attractive alternative, with significant improvements over the traditional cermet manufacturing methods [5]. SHS has been used for about 40 years and is an elegant and efficient method for producing a wide range of advanced materials [2, 5, 6]. Based on self-sustained exothermic reaction of the reactants, the method yields materials of high purity, because the high temperatures generated during the reaction cause any impurities to volatilize [2, 7]. Other than an ignition source, SHS does not require an external energy source or complex equipment, as the reaction is self-sustained energetically [7]. In fact, the power requirements of SHS are so low that it is one of the few methods of materials synthesis which is feasible in outer space [8]. In addition, the process is inexpensive and can be used to directly synthesize articles with a desired shape, size, and structure [7, 9]. The chemical reactions associated with SHS are typically completed in a few seconds, leading to the formation of the condensed product. Finally, the high reaction rates and relatively rapid cooling in SHS reactions can avoid

A. Nabavi · A. Capozzi · S. Goroshin · D. L. Frost (✉) ·
F. Barthelat (✉)
Department of Mechanical Engineering, McGill University,
817 Sherbrooke Street West, Montreal, QC H3A 0C3, Canada
e-mail: david.frost@mcgill.ca

F. Barthelat
e-mail: francois.barthelat@mcgill.ca

undesirable grain growth in products, which often occurs with conventional sintering methods [5, 7, 10].

A major drawback of materials obtained by SHS is their porosity, which results from several sources, including the porosity in the original reactants, gas evolution, molar change, and thermal migration during the reaction process itself [11, 12]. The traditional method for sample preparation in the SHS technique is to compact the reactant mixture powders to a typical density of about 80 % of the theoretical maximum density before igniting the mixture. This method requires a large compression force to increase the density of the reactive mixture and to minimize any pores in the green compact [2]. To eliminate porosity in the reactants, a new method for the preparation of the precursor charge of a metal–sulfur mixture is proposed in this study, which can be described as melt casting of a reactive mixture, or reactive casting in short. The porosity of the product material was experimentally measured, to verify the thermochemical prediction of low gas production during reaction and a dense final product. The quenching dimension (minimum size of sample which can sustain flame propagation despite heat losses) was also measured due to its critical importance to the ability to perform net-shape synthesis of complex shapes.

Thermochemical predictions

The thermodynamics of the Cr–S reaction ($\text{Cr} + \text{S} \rightarrow \text{CrS}$) was investigated using FactSage, a multiphase, multicomponent chemical equilibrium software package which includes extensive databases of known chromium–sulfur compounds and phases [13]. We computed the adiabatic flame temperature and amount of volumetric gas production (volume of gas at pressure normalized by volume of initial composition, giving an indication of the porosity of the final product) as a function of Cr:S molar ratio at various pressures, as shown in Figs. 1 and 2. These calculations predict that the reaction becomes completely gasless when the composition is stoichiometric (Cr:S molar ratio 1), at which point the adiabatic flame temperature peaks at 2333 °C. Increasing the Cr content beyond the stoichiometric value reduces the adiabatic flame temperature, while the reaction remains, in theory, gasless.

The phase diagram of the Cr–S system at a pressure of 1 atm is shown in Fig. 3 [14]. This diagram, in combination with the calculation of adiabatic flame temperature, indicates that the products of the synthesis are in the liquid state (prior to cooling and solidification) for the range of chromium-rich compositions studied in this paper ($1.0 \leq \text{Cr:S} \leq 4.0$), which is an advantageous property for net-shape synthesis.

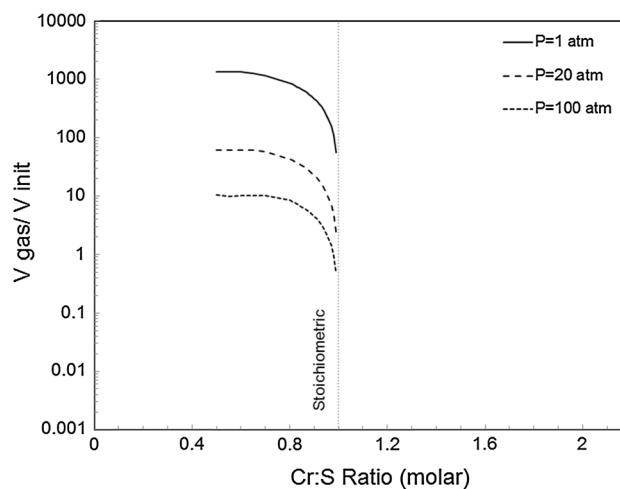


Fig. 1 Gas production as a function of Cr:S molar ratio

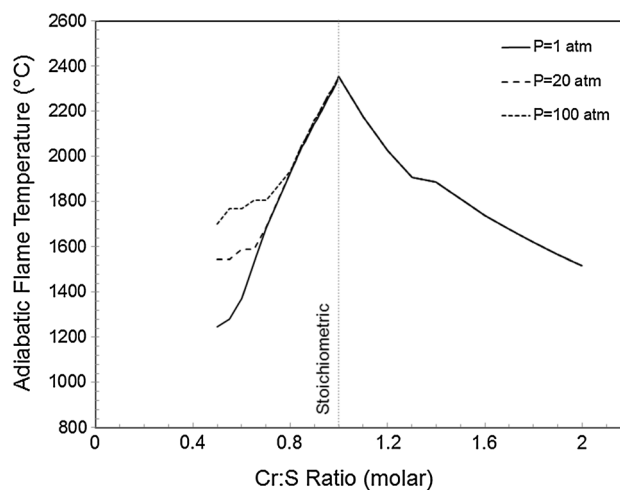


Fig. 2 Adiabatic flame temperature as a function of Cr:S molar ratio

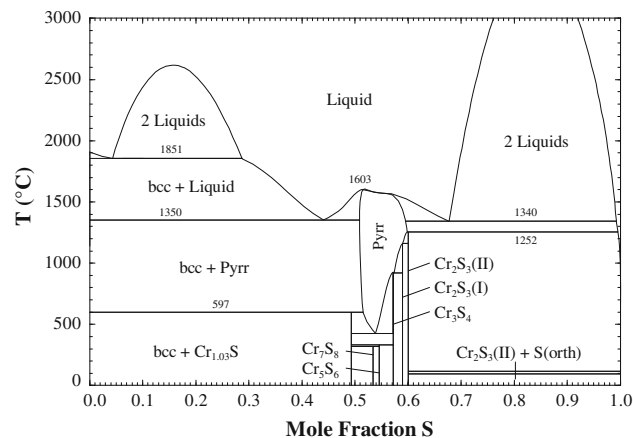


Fig. 3 Calculated optimized condensed chromium–sulfur phase diagram at a total pressure of 1 bar. *Pyrr* high-temperature chromium pyrrhotite, *S(orth)* solid pure sulfur with orthorhombic structure, and *bcc* body-centered cubic chromium solution phase [14]

Experimental procedure

The preparation of the reactive mixture used in this study is straightforward and may be described in a few steps (Fig. 6). The chromium powders used in the present work were obtained from Atlantic Equipment Engineers (NJ, USA). Two different Cr powders (99.8 % purity) were used: a fine powder with a particle size range given by the supplier of 1–5 μm (CR-102) and a coarse powder denoted –325 mesh, or nominally <44 μm (CR-103). Figure 4 shows SEM images and particle size distributions of the Cr powders, measured with a LA-920 Horiba laser scattering particle size analyzer. The CR-102 and CR-103 powders had average particle sizes, based on volume, of 3 and 26 μm , respectively. Sulfur powder with a purity of 99.5 % was obtained from Alfa Aesar (S4981, MA, USA). The average particle size was smaller than 150 μm (–100 mesh) but did not influence the fabrication process, since the sulfur was always melted to form the reactive mixture.

Chromium and sulfur powders were mixed in a roller mill, in the desired mass ratio. The powder mixture was heated in a mantle up to 160 $^{\circ}\text{C}$, which is slightly above the melting temperature for sulfur (temperature >120 $^{\circ}\text{C}$), but well below the melting temperature of chromium (1907 $^{\circ}\text{C}$). The molten mixture was then poured into a mold. No interaction between chromium and sulfur was observed at this step. Upon cooling of the reactive mixture, the sulfur solidified, forming a matrix of sulfur containing well-dispersed chromium inclusions (Fig. 5). This reactive mixture was then ignited at ambient pressure using an electrically heated tungsten wire embedded in the sample. The self-sustained flame propagated throughout the

sample, producing the final metal sulfide product (Fig. 6). Depending on the initial metal/sulfur molar ratio, some unreacted metal may remain in the product, yielding a ceramic–metal composite (cermet), as shown on Fig. 8.

Differential thermal analysis (DTA) using a standard LabsysTM instrument (Setaram Inc., France) was used to analyze the reactivity of chromium–sulfur mixture in the vicinity of the melting point of sulfur and beyond. The samples were prepared in accordance with the method developed in [15]. A small amount (5–12 mg) of ground reactive mixture of Cr–S (using fine Cr powder mixed with S with a stoichiometric ratio) was placed in a heavy-wall quartz capillary tube (2 mm OD, 1 mm ID), which was then flame-sealed from both ends (Fig. 7). The tube was

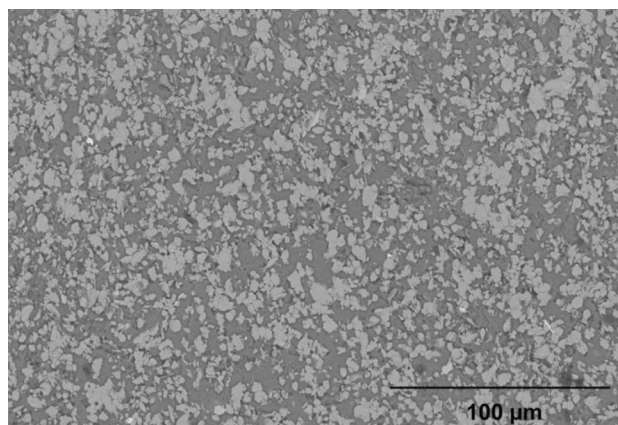
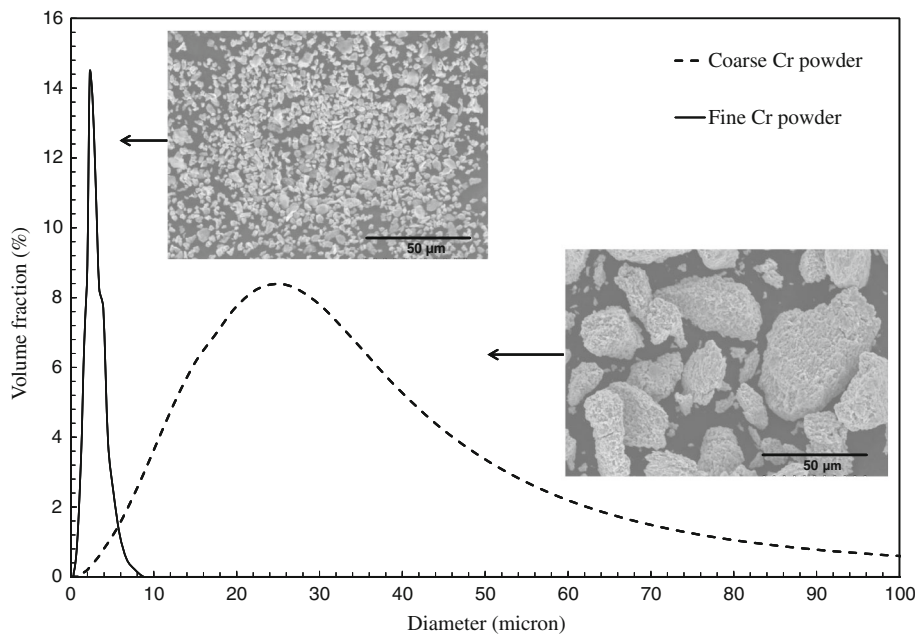


Fig. 5 SEM micrograph of the reactive mixture showing chromium particles (light tone) embedded in solidified sulfur matrix (darker tone). The distribution of the chromium particle was uniform

Fig. 4 Particle size distributions and SEM images of the Cr powders; fine powder (CR-102, with average particle size of 3 μm), and coarse powder (CR-103, with average particle size of 26 μm)



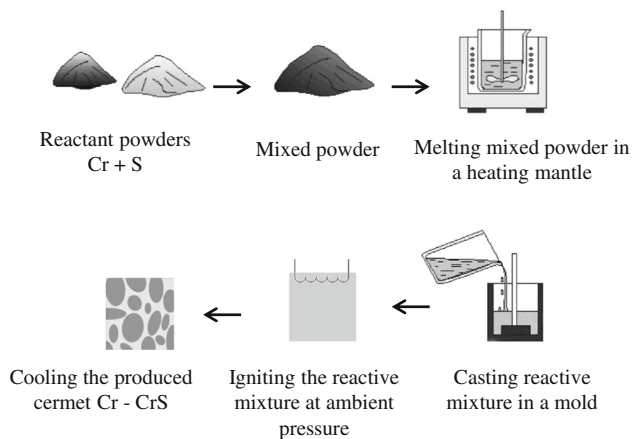


Fig. 6 Schematic of the manufacturing process

wrapped with a thin silver foil that formed a pedestal at the tube end and was placed vertically on the DTA platform. An equivalent, but empty, tube was used as a reference.

Fig. 7 DTA curve of Cr–S mixture and schematic of the flame-sealed quartz capillary with reactive Cr–S mixture

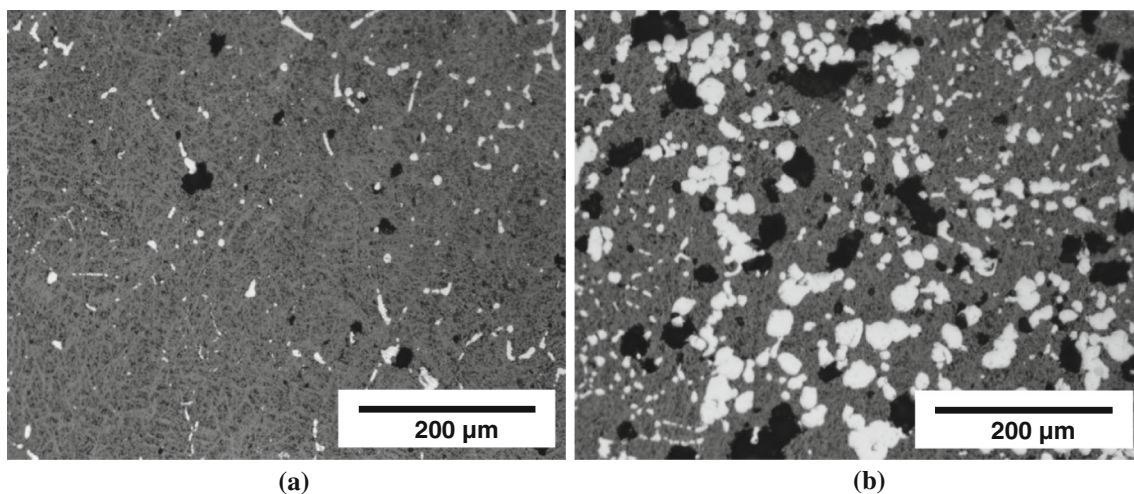
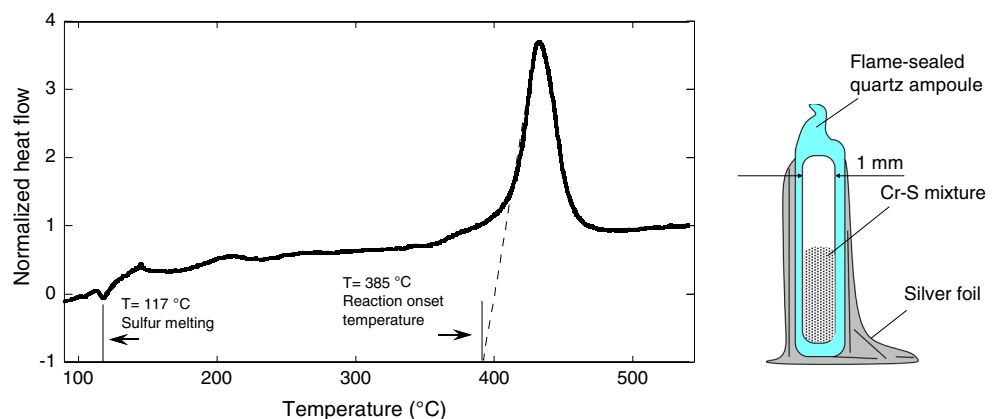


Fig. 8 Optical micrographs showing the microstructure of reacted samples with **a** fine Cr particles, and **b** coarse Cr particles, each with Cr:S molar ratio equal to 1. *Light* regions are residual Cr phase, *dark gray* regions are chromium sulfide, and *black* regions correspond to voids

The DTA instrument recorded the heat flow from the reactive mixture as a function of temperature. As can be seen from Fig. 7, the DTA curve for the Cr–S mixture exhibits two peaks; an endothermic reaction at a temperature of about 117 °C, corresponding to the melting point of sulfur, and an exothermic reaction with an onset temperature of about 385 °C which is near the ignition temperature of the Cr–S reaction. The reaction onset temperature recorded with the DTA is consistent with the ignition temperature of Cr–S mixture measured in other experiments by Goroshin et al. [16], using samples cast into a small cylindrical container and placed within a fiber heater, which was reported as 423 ± 7 °C.

Microstructure and composition

Optical microscopy and image analysis were used to examine the microstructure, phase size, and distribution of

the product samples. Specimens were cut, polished, and examined with a scanning electron microscopy (Hitachi S-3000N VP-SEM SEM) and energy dispersive spectroscopy (EDS). The density of the samples, before and after the reaction, was measured. The shape and distribution of the pores within the reacted specimens were determined using image analysis. Results show that the amount of residual Cr-rich phase in the produced cermet changes with the Cr particle size. Figure 8 shows the microstructure of two different samples with a Cr:S molar ratio equal to one, with two different Cr particle sizes. In the sample with coarse Cr particles (26 μm), there is a significant amount of residual Cr phase in the cermet. In contrast, the sample with similar composition, but finer Cr particles (3 μm), shows a relatively small amount of residual Cr phase in the cermet. Figure 9 shows the back-scattered electron (BSE) image of the microstructure of the sample synthesized with coarse Cr powder (26 μm), with a Cr:S molar ratio equal to 1. The energy dispersive X-ray (EDX) results show that the bright phases are residual Cr-rich phases, and the dark gray matrix is chromium sulfide, as tabulated in Table 1.

The X-ray diffraction (XRD) technique was used to determine the nature of the different phases which were formed during the synthesis or post-ignition process. Combustion-synthesized products with a Cr:S molar ratio equal to 1 were ground into fine powders and analyzed using copper K α 1 X-ray radiation to assess the phase constituents. XRD analyses showed Cr and CrS peaks, for both samples made from coarse and fine chromium powders (Fig. 10). Their XRD patterns are similar, with a slight difference in intensity of Cr peaks which are higher in the sample with coarse Cr particles compared with the sample with fine Cr particles. Also, according to the XRD patterns, there is sulfur remaining in the samples containing coarse Cr powder. These results indicate that the combustion synthesis is incomplete in the case of coarse Cr powder, as

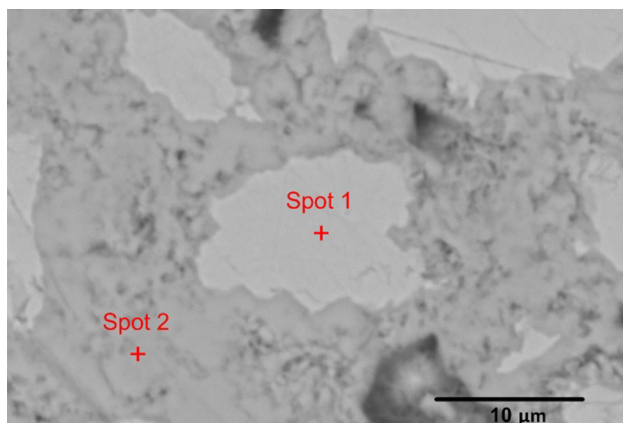


Fig. 9 BSE image of the microstructure of the sample synthesized with coarse Cr powder (26 μm), with Cr:S molar ratio equal to 1

Table 1 Chemical composition of the matrix and bright phase obtained from EDS point analysis

	Cr (wt%)	S (wt%)	O (wt%)	C (wt%)
Spot 1	86.80	4.75	3.61	4.84
Spot 2	55.20	32.31	2.78	9.72

indicated by the residual Cr-rich phase which was detected by XRD and observed with SEM in the final produced cermet. This is discussed in more detail in “[Particle size of reactants](#)” section below.

Product porosity measurement

Samples synthesized at ambient pressure had generally high porosity (as high as 70 %) with a large number of micro and macro cracks. The porosity was measured using image analysis, based on the ASTM E 562-02 standard test method [17] with the aid of Clemex, an image analysis software. Comparison of porosities before and after reaction indicates that the pores appeared during the reaction. High porosity represents a significant obstacle to the use of the cermet in structural applications, and we therefore carefully investigated its possible sources in order to suppress it. Potential sources of porosity include impurity-generated porosity, porosity existing within the starting powders and reactive mixture, porosity generated by sulfur vaporization within the flame front, expansion of pre-existing closed pores within the reactive mixture after reaction, and porosity from molar volume changes. The following sections describe how the manufacturing process was modified in order to address these problems and minimize porosity.

Vacuum degassing of the melt before ignition

Adsorbed water, low boiling-point impurities, and dissolved hydrogen on the surface of powders prior to SHS are possible sources for impurity-generated porosity in SHS products. Due to the high combustion temperatures, these impurities are volatilized as the wave propagates through the reactants during the SHS process [11, 18]. Therefore, the best way to reduce these sources of porosity is to use highly purified initial powders which can eliminate or significantly reduce the formation of impurity-generated porosity, as well as vacuum degassing the molten mixture to remove trapped gases before ignition. By vacuum degassing of the molten mixture, the porosity in the solidified precursor reactive mixture was reduced to 3 %, eliminating the round, bubble-like pores (gas pores).

Fig. 10 XRD patterns of samples fabricated with fine (1–5 μm) and coarse (<44 μm) Cr powders, both with Cr:S molar ratio equal to 1

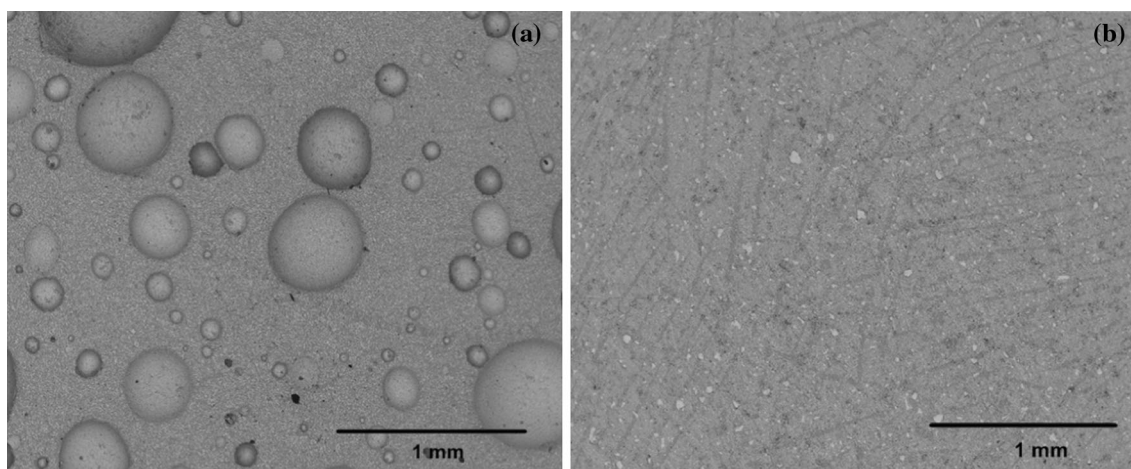
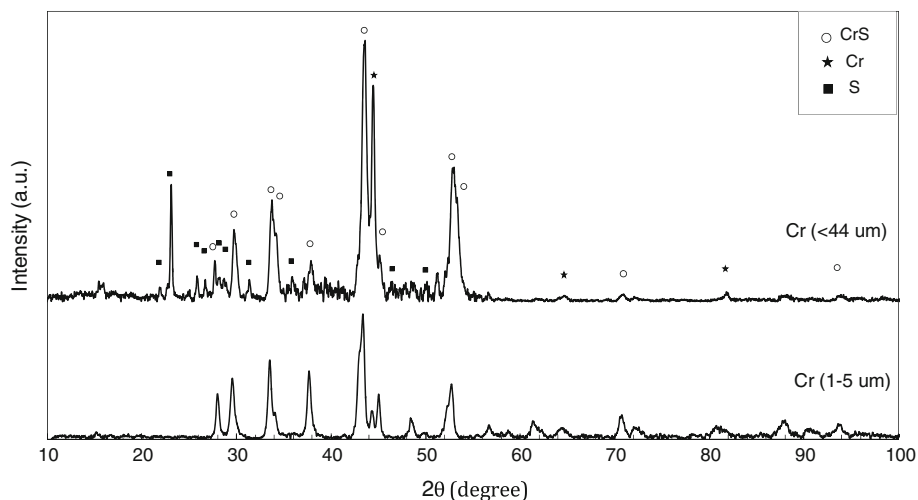


Fig. 11 Backscattered electron images showing reactive mixture; **a** without vacuum degassing, **b** with vacuum degassing (same composition)

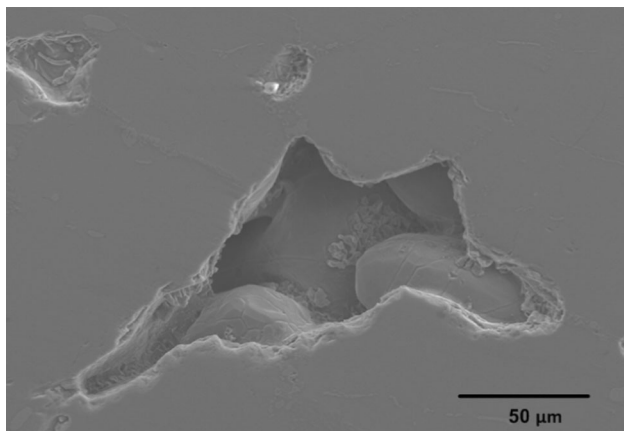


Fig. 12 Secondary electron image showing grain separation during solidification

Figure 11 shows BSE images from reactive mixtures with and without vacuum degassing. The remaining pores in the cermet after degasification appear more elongated, and

when observed with SEM, it appears as if the grains were pulled apart during solidification (Fig. 12).

Particle size of reactants

With the use of coarse Cr powder, both the microstructure and the XRD patterns (Figs. 8, 10) show that the combustion synthesis was incomplete, because residual Cr-rich phase was detected by XRD and observed with SEM in the final product. The incompleteness of the combustion reaction may be explained by the coarseness of the Cr powder, since a negligible amount of residual Cr-rich phase could be seen in the combustion-synthesized product with fine Cr powder. Smaller reactant particles may lead to the different degree of completeness of the reaction, because a higher surface to volume ratio for the powder, with more contact surfaces and shorter distances for the sulfur atoms to diffuse to the chromium particles. If the reaction is

incomplete, sulfur will remain unreacted inside the sample. The remaining sulfur might then vaporize because of the high temperature of the reaction and may lead to further porosity generation [19, 20].

Theoretically, there should be no remaining Cr and S, when the composition is stoichiometric (Cr:S molar ratio 1). However, the Cr remaining indicates that some of the sulfur has also remained and therefore vaporized during the reaction. Also, in Fig. 10, the XRD patterns show there is sulfur remaining in the samples containing coarse Cr powder.

This explains why the cermet produced with coarse Cr powder is more porous than the cermet made with fine Cr powder, with the same composition (Fig. 8 in “[Microstructure and composition](#)” section). Consequently, finer Cr powders are preferable, but there is a limit imposed by the requirement for the molten composition to be fluid enough to be melt-cast. Large particle sizes produce a fluid-like rheology in the melt, while the very fine Cr particles result in a thick, paste-like composition. It is difficult to remove trapped gases from highly viscous melts by vacuum degassing.

Preheating of the mold

In order to fill the mold more easily without producing any pores in the reactive mixture, the mold should be preheated to a temperature near the melting point of sulfur to avoid the sudden solidification of the reactive mixture.

Static pressure

The amount of gas products strongly depends on the hydrostatic pressure during the reaction (Fig. 1). Higher static pressure of the inert gas atmosphere in which the synthesis is conducted can reduce gas formation by suppressing the vaporization of sulfur and other nonequilibrium processes that may occur within the flame reaction zone. In addition, increased pressure decreases the relative volume occupied by gases that are evolved, further reducing the porosity. Experimentally, the porosity of the product synthesized with a Cr:S molar ratio of 1.15 was measured following synthesis in a high-pressure reactor pressurized with argon and is reported in Fig. 13(b). The

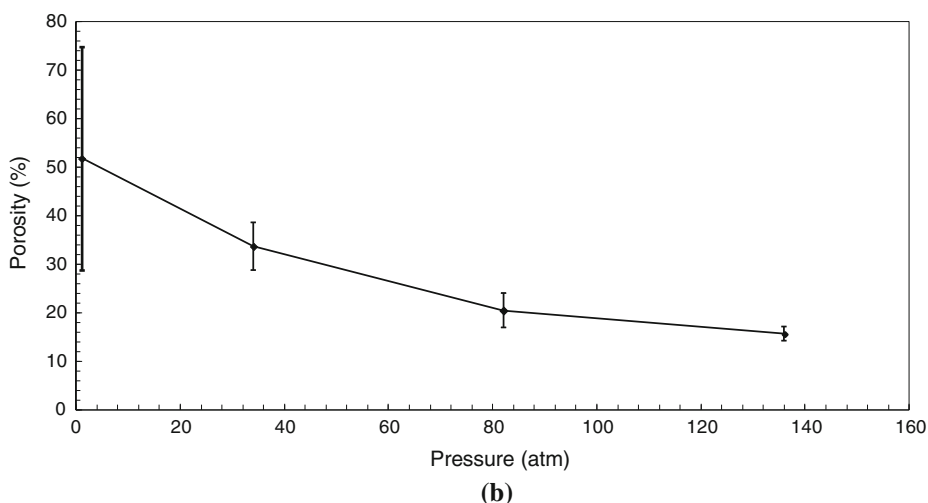
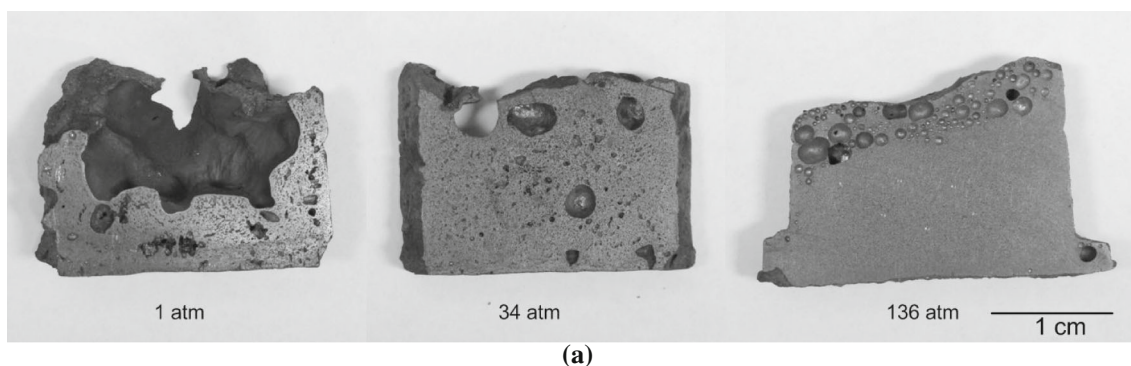


Fig. 13 **a** Cut samples which were synthesized at three different pressures, and **b** Porosity as a function of static pressure at which the synthesis was conducted

porosity was determined via analysis of the images. Increasing static pressure has a visible effect of reducing the porosity, as shown on Fig. 13a. All samples were synthesized with a Cr:S 1.15 molar ratio and with fine Cr powder ($3\ \mu\text{m}$).

Increasing the static pressure at which the synthesis occurs to 136 atm leads to a reduction in the porosity of the product to below 14 %. However, an additional increase in the pressure above 136 atm does not appear to significantly reduce the porosity further.

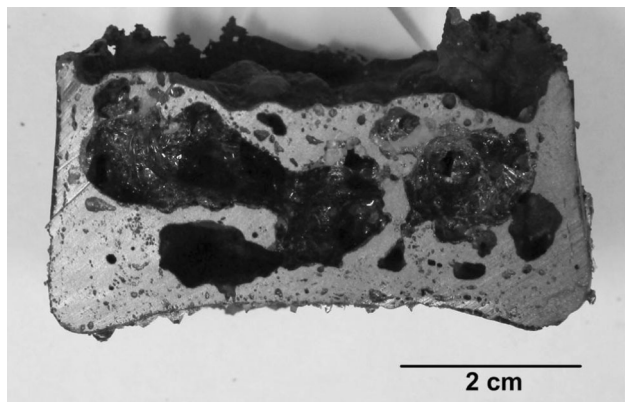


Fig. 14 Cut sample which was ignited under vacuum

Vacuum degassing during synthesis

We also investigated the effect of applying vacuum during the synthesis process. For this part of the investigation, the samples were ignited in the molten state, and were synthesized with a Cr:S 1.15 molar ratio and with fine Cr powder ($3\ \mu\text{m}$). The samples produced had large pores and were almost as porous as the samples first ignited at ambient pressure (Fig. 14). Vacuum degassing during the synthesis process did not appear to decrease the porosity or improve the quality of the final product.

Directional solidification

As stated above, there were many micro and macro cracks in the samples produced. In addition, in some samples, there were central cracks and voids (Fig. 15a). Figure 15b also shows BSE images of the micro and macro cracks in samples which were synthesized under 136 atm with a Cr:S 1.15 molar ratio and with fine Cr powder ($3\ \mu\text{m}$). These cracks might be a result of thermal shock due to the high cooling rate in SHS (10^3 – $10^6\ \text{°C/min}$). Most metals and alloys shrink when they change from a liquid to a solid state [21]. As a result, a shrinkage defect will form, when the solidification is governed by progressive solidification over directional solidification.

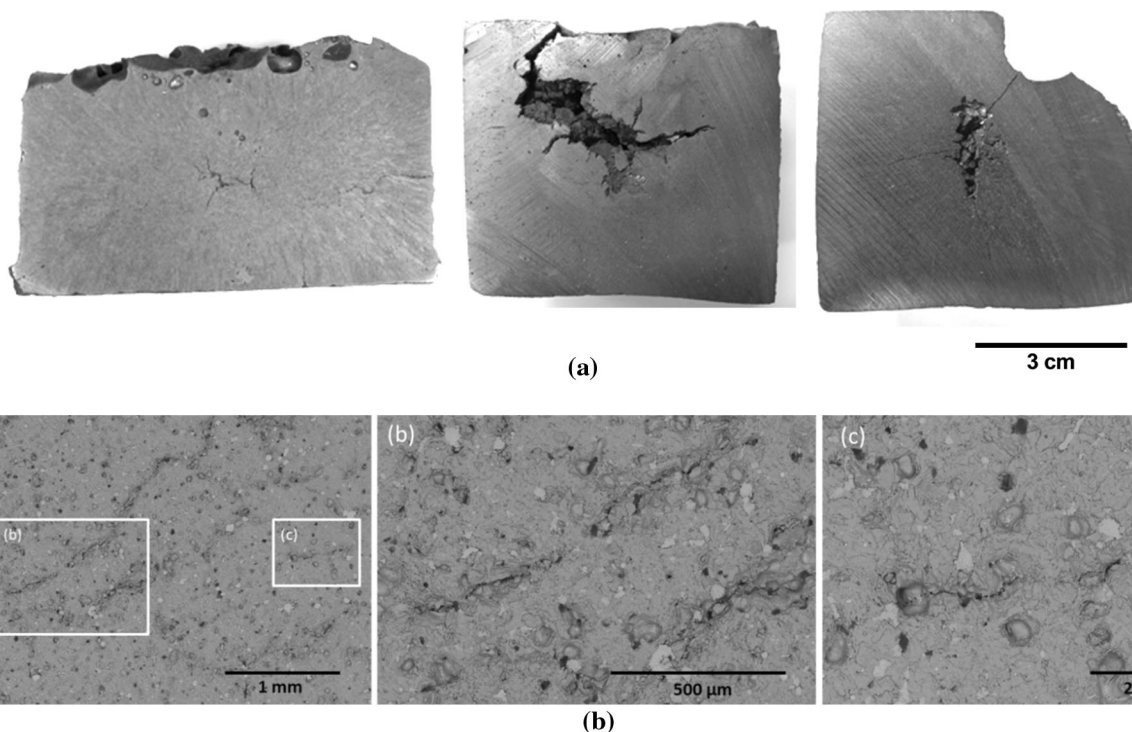


Fig. 15 **a** Cut samples which show central void and cracks, and **b** BSE image of the micro and macro cracks in produced sample synthesized under 136 atm with Cr:S 1.15 molar ratio and with fine Cr powder ($3\ \mu\text{m}$)

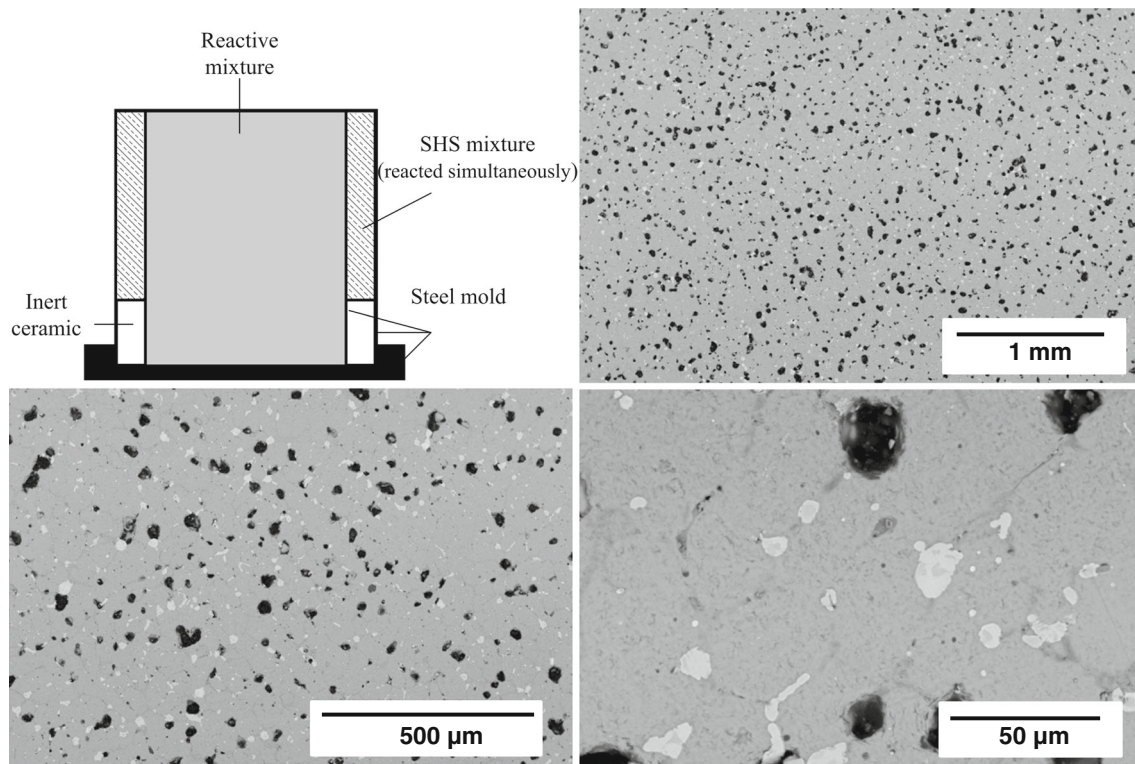


Fig. 16 Schematic representation of directional solidification method, and SEM images from a produced sample by directional solidification method in different magnifications

Directional solidification is achieved by a one-dimensional thermal flux along the sample axis and sufficient heat exchange between the sample and cooling medium. Therefore, in order to prevent cracks and voids from developing, we developed a method to cool the samples slowly and directionally after the reaction. Figure 16 shows a schematic of the directional solidification method in which a jacket of SHS mixture was cast on top of a shallow layer of inert ceramic. This prevented heat loss from the top of the sample, while allowing a small amount of heat to transfer through the inert ceramic, and a greater amount of energy to escape through the base of the steel mold. The solidification front therefore moves in a unidirectional manner from bottom to top. This modification successfully suppressed crack formation (Fig. 16).

Supercritical sulfur

Because of the high temperature of the reaction, it is possible that some pores may be generated by vaporization of sulfur in the flame front. Also, if sulfur gas was produced rather than consumed during combustion, the existence of sulfur may lead to additional generation of porosity, in a manner similar to the effect of impurity evolution. Since there is no distinction between liquid and gas phases above

the critical point, in the next step, the sample was ignited above the liquid–vapor critical point of sulfur, such that sulfur as a homogenous supercritical fluid. The critical temperature and pressure for sulfur are 1041 °C and 207 atm, respectively. The result was promising, and the porosity of produced cermet decreased to about 7 %. Figure 17 shows BSE images with different magnifications from a sample produced with the directional solidification method with supercritical sulfur (Cr:S 1.15 molar ratio and with fine Cr powder (3 μm)).

Thus, in the modified manufacturing process (shown schematically in Fig. 18), the particle size of the reactants was considered. Then, the molten mixture of Cr and S powders was degassed in a vacuum chamber (vacuum pressure = 95 kPa) for about 20 min and at high temperature to maintain sulfur in a molten state. After that, it was poured into a preheated mold to prevent contact solidification of the melt. The solidified reactive mixture was then placed in a pressurized reactor and ignited in a high-pressure inert gas (Ar) environment, using an electrically heated tungsten wire embedded in the sample. By igniting the sample above the liquid–vapor critical point of sulfur, and cooling the samples slowly and directionally after the reaction, the porosity inside the produced cermets was reduced to about 7 %, and no cracks were observed inside the cermets (Fig. 17).

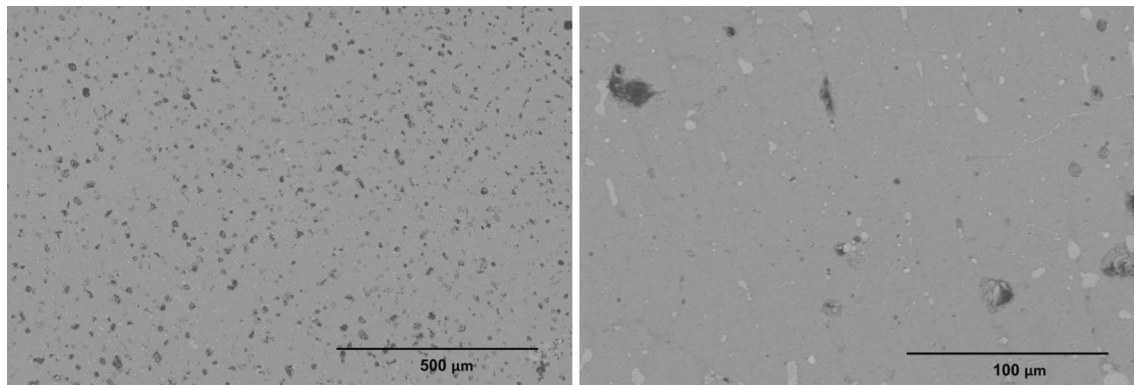
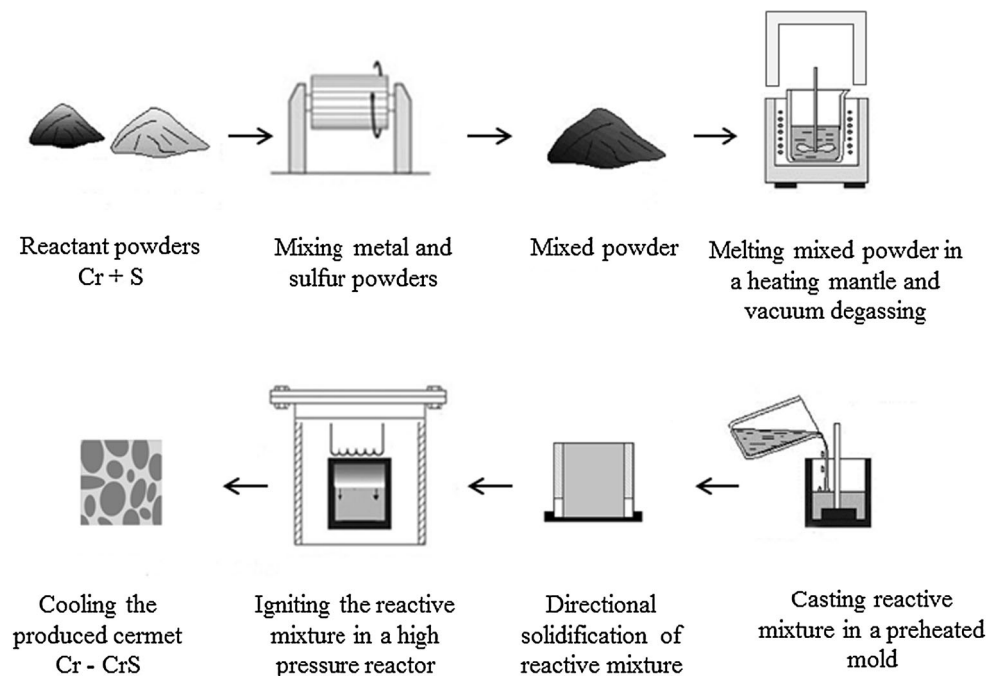


Fig. 17 SEM images from a produced sample by directional solidification method with supercritical sulfur in different magnifications

Fig. 18 Schematic of the modified manufacturing process



Combustion front quenching test

As mentioned above, we have introduced and investigated a new method for producing metal sulfide cermets to enable the possibility to perform net-shape synthesis of dense, near theoretical density product. By improving the manufacturing process, we were able to produce a dense cermet with no cracks. Then, in the next step, we evaluated the possibility of net-shape manufacturing of these cermets by measuring the quenching thickness.

Quenching thickness is the minimum size of sample that can sustain flame propagation with heat loss and is one of the fundamental measurements that can be made in a reactive material. Measurement of quenching thickness is of critical importance to the ability to perform net-shape synthesis of complex shapes. Therefore,

we measured the quenching thickness of Cr–S mixtures to investigate the lower limit for the thickness of the sample.

To measure the quenching thickness, a rectangular (slab) charge was cast in a brass channel of 1 cm width and a charge thickness that decreased in successive steps as shown in Fig. 19. The flame was initiated in a large reservoir of mixture and then entered the test section, encountering successively smaller charge thicknesses. These tests were performed at ambient pressure (1 atm). The location of quenching was easily identified by melting away the unreacted mixture as well as the visual difference of appearance between the reactant and product upon recovery of the sample.

The results showed that Cr–S mixtures using the fine Cr powder (3 μm) did not quench in even the smallest channel

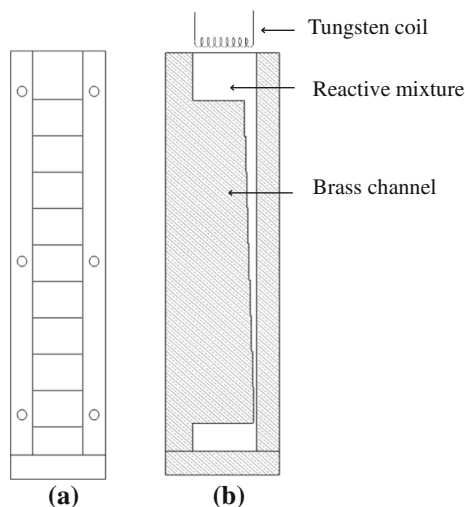


Fig. 19 Drawing of the **a** channel (*front view*), **b** combustion front quenching test (*side view*)

thickness, successfully propagating in channels as small as 0.6 mm. It was also found that the quenching dimension did not have a strong dependence on the Cr:S ratio. Therefore, it can be concluded that regardless of the chemical composition of the mixture, Cr–S mixtures have very small quenching thicknesses which enables us to perform net-shape synthesis of CrS–Cr cermet with sub-millimeter scale features.

Conclusions

In this paper, we demonstrated the ability of the melt-casting SHS technique to produce near theoretical density chromium/chromium sulfide ceramic–metal composite (cermet) articles of a desired shape. Although thermodynamics predicts that no gas is produced during the reaction for a Cr-rich formulation, synthesis performed at ambient pressure resulted in a product with considerable porosity. The use of a degassed, melt-cast reactive mixture with excess chromium, and performing the synthesis under high pressure has been shown to be the essential requirements to minimize porosity. The ability of the Cr–S system to sustain propagation in small dimension charges, with a quenching distance less than 1 mm with fine Cr powder, implies that the technique developed here can be used for net-shape synthesis of complex shapes with high tolerances. With the various improvements to the manufacturing process, the porosity was reduced from 70 to 7 %. This level of porosity obtained is considerably less in comparison with samples produced by other SHS techniques and is comparable to the bulk form of industrially manufactured ceramics [11]. This residual porosity may be attributed to the release of gases evolved by impurities (oxides,

moisture, etc.) and the “freezing” of porosity caused by nonequilibrium evolution of gases during the combustion process. Chromium sulfide is also denser than the initial reactive mixture and the liquid sulfide product, which results in shrinkage-induced gaps and pores in the final product. The density of the samples was measured for 8 different samples with a Cr:S molar ratio equal to 1.15, before and after the ignition. The values obtained were 3.78 ± 0.01 g/cc for the reactive precursor mixture compared with 4.04 ± 0.05 g/cc for the cermet produced.

This novel method simplifies the preparation of samples with different shapes, thicknesses, and with a green density close to theoretical density. It also eliminates trapped gases within the reactive mixture, improving the quality of the synthesized product, and homogeneity of the product structure. Cermet samples produced by this method can be used as ballistic armors, heating elements, protective coatings to resist corrosion from liquid metals, and magnetic structures.

Acknowledgements This work was supported by a Strategic Grant from the Natural Sciences and Engineering Research Council of Canada. Atefeh Nabavi was partially supported by a McGill Engineering Doctoral Award. The authors would like to thank Prof. In-Ho Jung for his contributions to the thermochemical calculations. Input from Prof. Andrew Higgins is also gratefully acknowledged.

References

- Plichta EJ, Behl WK (1995) Cathode material for use in a high temperature rechargeable molten salt cell and high temperature rechargeable molten salt cell including the cathode material. US Patent H001397
- Mizera MA (1997) Ignition temperature measurements of metallic sulfides in SHS processes. McGill University, Montréal
- Jellinek F (1957) The structures of the chromium sulphides. *Acta Crystallogr A* 10(10):620–628. doi:10.1107/S0365110X5702200
- Mrowec S, Zastawnik M (1966) On the defect structure of chromium sulphide. *J Phys Chem Solids* 27(6–7):1027–1030. doi:10.1016/0022-3697(66)90075-8
- Fu Z, Wang H, Wang W, Yuan R, Munir Z (1992) Process of study on self-propagating high-temperature synthesis of ceramic-metal composites. *Int J SHS* 2(175):1993a
- Varma A, Lebrat J-P (1992) Combustion synthesis of advanced materials. *Chem Eng Sci* 47(9):2179–2194
- Zhang WN, Wang HY, Wang PJ, Zhang J, He L, Jiang QC (2008) Effect of Cr content on the SHS reaction of Cr–Ti–C system. *J Alloy Compd* 465(1–2):127–131. doi:10.1016/j.jallcom.2007.10.092
- James W (ed) (1998) *Advances in chemical engineering*, vol 24. Academic Press, New York. doi:10.1016/S0065-2377(08)60087-3
- Merzhanov AG (2004) The chemistry of self-propagating high-temperature synthesis. *J Mater Chem* 14(12):1779–1786
- Gennari S, Tamburini UA, Maglia F, Spinolo G, Munir ZA (2006) A new approach to the modeling of SHS reactions: Combustion synthesis of transition metal aluminides. *Acta Mater* 54(9):2343–2351. doi:10.1016/j.actamat.2006.01.009
- Munir Z (1993) Analysis of the origin of porosity in combustion synthesized materials. *J Mater Synth Process* 1(6):387–394

12. Munir Z, Wang L (1990) The contribution of thermal migration to pore formation during SHS reactions. In: Kaieda Y, Holt JB (eds) Proceedings of first US-Japanese workshop on combustion synthesis, National Research Institute for Metals, pp 123–137
13. Bale C, Chartrand P, Degterov S, Eriksson G, Hack K, Ben Mahfoud R, Melançon J, Pelton A, Petersen S (2002) FactSage thermochemical software and databases. CALPHAD 26(2): 189–228
14. Waldner P, Sitte W (2011) Thermodynamic modeling of the Cr–S system. Int J Mater Res 102(10):1216–1225
15. Jones DE, Augsten RA (1996) Evaluation of systems for use in DSC measurements on energetic materials. Thermochim Acta 286(2):355–373
16. Goroshin S, Miera A, Frost D, Lee J (1996) Metal–sulfur combustion. In: Symposium (international) on combustion, vol 2. Elsevier, Amsterdam, pp 1883–1889
17. ASTM Standard E 562-02: Standard Test Method for Determining Volume Fraction by Systematic Manual Point Count (2002). ASTM International, West Conshohocken
18. Morsi K, Shinde S, Olevsky E (2006) Self-propagating high-temperature synthesis (SHS) of rotator mixed and mechanically alloyed Ni/Al powder compacts. J Mater Sci 41(17):5699–5703. doi:[10.1007/s10853-006-0068-x](https://doi.org/10.1007/s10853-006-0068-x)
19. Shibuya M, Ohyanagi M, Munir ZA (2002) Simultaneous synthesis and densification of titanium nitride/titanium diboride composites by high nitrogen pressure combustion. J Am Ceram Soc 85(12):2965–2970. doi:[10.1111/j.1151-2916.2002.tb00564.x](https://doi.org/10.1111/j.1151-2916.2002.tb00564.x)
20. Kanetake N, Kobashi M (2006) Innovative processing of porous and cellular materials by chemical reaction. Scripta Mater 54(4):521–525. doi:[10.1016/j.scriptamat.2005.10.063](https://doi.org/10.1016/j.scriptamat.2005.10.063)
21. Campbell JCJESP (2003) Castings. Butterworth Heinemann, Oxford